Appl. Phys. A 29, 213–217 (1982)

Applied Physics A Solids and Surfaces

Error Sources for the Analysis of Doppler Broadening in Positron Annihilation Spectra

D. Otero and A. N. Proto

Departamento de Física, Comisión Nacional de Energía Atómica Av. del Libertador 8250, RA-1429 Buenos Aires, Argentina, and
Departamento de Física, Facultad de Ciencias Exactas, Universidad Nacional del Centro de la Provincia de Buenos Aires, Pinto 399, RA-7000 Tandil, Argentina

R. Romero and A. Somoza*

Departamento de Física, Facultad de Ciencias Exactas, Universidad Nacional del Centro de la Provincia de Buenos Aires, Argentina

Received 29 January 1982/Accepted 2 August 1982

Abstract. Correction factors for systematic shifts of the second-order moment σ^2 (linearly related to S^{-1}) of the Doppler broadened annihilation gamma ray lineshape are presented. They allow to compare σ^2 values obtained under different experimental conditions. The height of the observed peak, the number of keV/channels used and the number of channels over which the Doppler broadening dsstribution should be considered are bounded by the "a priori" settled relative uncertainty of σ^2.

PACS: 72.15

Positron annihilation studies have become a powerful tool in the inference of the electron density and momentum distribution of condensed matter. The variety of applied techniques and their possibilities are outlined in [1, 2].

When the observation of the annihilation gamma rays is made through a Ge(Li) detector, the 511-keV peak appears significantly broadened, because it contains two convoluted contributions:

a) the natural response shape of the detector to monochromatic gamma rays and *b)* the intrinsic Doppler broadening.

The latter contains the relevant information about the momentum of the annihilation pair and should be obtained from the total measured distribution.

Several solutions have been attempted to get the desired intrinsic Doppler broadening.

Summarizing they are:

i) Deconvolution: the observed folded distribution of the 511-keV gamma rays, $F(x)$, is considered as a first class Fredholm equation given by

$$F(x)=\int_{-\infty}^{\infty} f(x-x')g(x')dx', \tag{1}$$

where $f(x)$ is the intrinsic Doppler distribution and $g(x)$ is the response function of the detector. The intrinsic $f(x)$ distribution is obtained unfolding the observed $F(x)$ distribution with the response $g(x)$ function [3, 4].

ii) Line-shape parameter: it is an empirical parameter defined by [5, 6]

$$S=\frac{\sum_{-C}^{C} Y_i}{\sum_{i=-B}^{-A} Y_i+\sum_{i=A}^{B} Y_i}, \tag{2}$$

where the subindex i is the channel number, Y_i are the counts per channel, $\pm C$ points the upper and lower channel near the middle of the peak and $\pm A$, $\pm B$ label channels at left and right tails of the peak, respectively. As it was pointed out in [5] there is no unified criterion about its extension and even about the definition of S. An alternative parameter is the variance (σ^2) of the Doppler broadening distribution and it was demonstrated [6] that there exists a linear relation between S^{-1} and σ^2.

* Fellow of the CIC, PciA Bs. As., Argentina

0721-7250/82/0029/0213/$01.00

In this work we intend to evaluate the statistical and systematic errors of σ^2 introduced by taking a finite interval around the distribution (defined from $-\infty$ to $+\infty$) and by considering discrete sets of values. Besides, we propose several criteria to choose the appropriate interval to get the desired information.

1. Generalities

Equation (1) could be formally expressed as

$$F(i)=\sum_{-\infty}^{\infty} f(j-i)g(j), \tag{3}$$

where we associate a discrete i variable (channel number) to the continuous x variable.
The centered and normalized moments of $F(i)$ follow the relations [7]

$$M_F^{(2)}=M_f^{(2)}+M_g^{(2)}, \tag{4a}$$

$$M_F^{(3)}=M_f^{(3)}+M_g^{(3)}, \tag{4b}$$

$$M_F^{(4)}=M_f^{(4)}+M_g^{(4)}+6M_f^{(2)}M_g^{(2)}. \tag{4c}$$

In cases where the positron thermalization is probably not complete, like in gases or low-density materials, the first and third order moments will give the direction (with respect to the positron source) of incomplete thermalization.
Instead, the second and fourth order moments will provide information on symmetrical changes in the distribution shape.
In the analysis of gamma ray spectra it is usual to assume well-known functions to describe analytically the shape of the peak. To describe the response function for monochromatic gamma rays we introduce:
i) a Gaussian shape for the upper half of the peak: $g(i)\sim e^{-i^2/2\sigma^2}$,
ii) exponential tails on each side of the peak, with the function and its derivative both matched to the Gaussian shape: $g(i)\sim e^{-\lambda_{L,R}i}$, where L and R correspond to left and right tails and $\lambda_L>\lambda_R$.
We assume that the intrinsic $f(i)$ distribution is composed by a parabolic component plus Gaussian tails (we only consider metals) [1, 2].
The former represents the contribution of the conduction electrons to the annihilation process and the latter rises from the core electrons. Naturally, $F(i)$ is the convolution of $f(i)$ and $g(i)$.
It is a well known mathematical method [7] to obtain information about a given distribution through the evaluation of the moments. However, to use them properly in the evaluation of an experiment, it is also necessary to calculate the associate errors. From (4a) we see that

$$\Delta(M_F^{(2)})\simeq\Delta(M_f^{(2)})+\Delta(M_g^{(2)}), \tag{5}$$

where $\Delta(M_\alpha^{(2)})$ means, "error of the second order moment of the $\alpha(i)$ distribution" and under this symbol we include both, statistical and systematic errors.
The object of this paper is then to evaluate $\Delta(M_f^{(2)})$ from the two measured $F(i)$ and $g(i)$ distributions.

2. Error Calculations

2.1. Second-Moment Error Calculation of the g(i) Response Function

For $g(i)$ response function we consider a) statistical and b) systematic errors. Then,

$$\Delta(M_g^{(2)})\simeq|\delta(M_g^{(2)})|+\varepsilon(M_g^{(2)}), \tag{6}$$

where $\delta(M_g^{(2)})$ and $\varepsilon(M_g^{(2)})$ are the above mentioned components, respectively.
a) Statistical Errors. Following the usual error propagation for the $M_g^{(n)}$ moments we get for the $g(i)$ distribution

$$(\delta M_g^{(n)})^2\sim\sum_i\left[i^{2n}+\left(\frac{n^2i^{2n-2}g^2}{\left(\frac{\partial g}{\partial i}\right)^2}\right)\right](\delta g)^2, \tag{7}$$

where i is the channel number, n the order of the moment and δg means the statistical error of $g(i)$. The first term of the right-hand side corresponds to the statistical error of counts per channel; the second is due to the correlation between the channel and its number of counts given by the shape of the measured peak.
We set, for (7), the external condition that the latter term will be of the same order as the former, as it seems to be an adequate choice.
This, and the assumption that $g(i)\simeq h\,e^{-\lambda i}$ (for $i>1/\lambda$) gives

$$i\sim n/\lambda. \tag{8}$$

Besides we need $|\partial g/\partial i|>\delta g$ in order to have a well defined derivative and then using (7) and (8)

$$n<\ln(h\cdot\lambda_D), \tag{9}$$

where h is lower than the height of the distribution, and then (9) is a suitable upper limit for the order of the moment under consideration.
We have used λ_D in (9) as it gives the more restrictive condition for the order of the moment, n, according to our requirement of having a well defined derivative $\partial g/\partial i$ with respect to the statistical error δg.
b) Systematic Errors. The change from the continuous x variable to the discrete i variable in (3) originates a systematic error.

It could be estimated through the Sheppard correction [8] given by

$$M^{(2)}=\bar{M}^{(2)}-\delta i^2/12, \tag{10a}$$

$$M^{(3)}=\bar{M}^{(3)}, \tag{10b}$$

$$M^{(4)}=\bar{M}^{(4)}-\tfrac{1}{2}\bar{M}^{(2)}(\delta i)^2+\tfrac{7}{240}(\delta i)^4, \tag{10c}$$

where δi is the width of the partition. If we call ε the relative error of $\delta i^2/12$ over $M^{(2)}$ we obtain from (10a)

$$\delta i<1.474\,\varepsilon^{1/2}\,R, \tag{11}$$

where the detector resolution R is, as it is well known, approximately equal to $R\simeq 2.35\,[M^{(2)}]^{1/2}$ assuming a Gaussian shape.

Equation (11) sets a condition on the number of keV/channel necessary to minimize the error introduced by using a discrete variable.

From (10c) we see that the same δi value doubles the relative error for $M^{(4)}$ in comparison with that of $M^{(2)}$ if we assume a Gaussian shape and then $\gamma_2=M_f^{(4)}/(M_f^{(2)})^2=3$ [8] (only the negative term is an important one).

Another important systematic error results from the fact that it is not possible to extend the summation limits to $\pm\infty$. Instead, a finite interval $[-\mathrm{B}, \mathrm{A}]$ is commonly used. Then, the second-order moment can be written as

$$M^{(2)}=\sum_{-\mathrm{B}}^{\mathrm{A}} i^2 g(i)+\varepsilon_g=\hat{M}_g^{(2)}+\varepsilon_g(R,\lambda,\mathrm{B},\mathrm{A}), \tag{12}$$

where $\hat{M}$ means finite summation limits in the computation of the moments.

To evaluate ε_g we suppose that the channels corresponding to $-\mathrm{B}$, A were located on both tails of the peak where it is possible to assume, as usual, $g(i)\sim\exp(-\lambda i)$. Then, the error $\varepsilon_g(R,\lambda,\mathrm{B},\mathrm{A})$ due to finite interval consideration could be expressed as

$$\begin{aligned}\varepsilon_g(R,\lambda,\mathrm{B},\mathrm{A})=\varepsilon_g&=M_g^{(2)}-\hat{M}_g^{(2)}\\&=\sum_{-\infty}^{-\mathrm{B}} g(i)i^2+\sum_{\mathrm{A}}^{\infty} g(i)i^2.\end{aligned} \tag{13}$$

The functional form of both summations is the same. Defining $i_{\mathrm{B}}^g\lambda=\chi_g$, where i_{B}^g is the value of the channel at point B for the $g(i)$ distribution, we obtain for the left-hand side

$$\sum_{\mathrm{B}}^{-\infty} g(i)i^2=\varepsilon_g^{\mathrm{B}}=\Psi_{\mathrm{B}}\frac{\eta(\chi_g)}{\sigma_g}, \tag{14}$$

where

$$\eta(\chi_g)=\mathrm{e}^{-\chi_g}(\chi_g^2-2\chi_g+2) \tag{15}$$

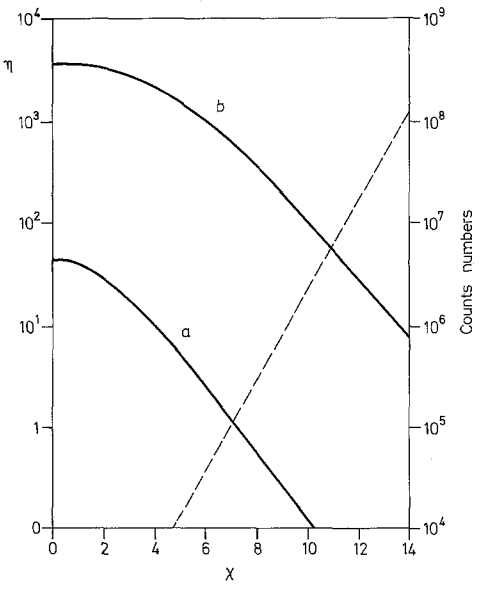

Fig. 1. The solid curves represent the η functions for the second order a and the fourth order b moments plotted against a generalized x coordinate. The scale is on left-hand side. The dashed curve gives the relation between h_0 and the x coordinate under the condition $\ln h_0>x+2\ln\lambda$, see (8) and (9), for a Ge(Li) detector with $1/\lambda=2.4$ keV and $\Delta i\sim 0.24$ keV/channel. Scale on right-hand side.

and Ψ_{B} is a normalization function which will be evaluated in the following paragraphs. In Fig. 1 a plot of $\eta(\chi)$ vs. χ is shown.

Experimentally we can obtain $\Delta\varepsilon_g^{\mathrm{B}}$ as the result of evaluating $\varepsilon_g^{\mathrm{B}}$ at two different cutting points, then

$$\Delta\varepsilon_g^{\mathrm{B}}={}_{(2)}\hat{M}_g^{(2)}-{}_{(1)}\hat{M}_g^{(2)}, \tag{16}$$

where ${}_{(\alpha)}\hat{M}_g^{(2)}$, with $(\alpha)=1,2$, means the second-order moment evaluated at ${}_{1,2}i_{\mathrm{B}}^g=\chi_g^{1,2}$ points for the left-hand side of the $g(i)$ distribution. Then, from (16) we get

$$\Delta\varepsilon_g^{\mathrm{B}}=\Psi_{\mathrm{B}}\left(\frac{\eta(\chi_g^{(2)})}{\sigma_g}-\frac{\eta(\chi_g^{(1)})}{\sigma_g}\right). \tag{17}$$

As the left-hand side is experimentally obtained and the parenthesis could be calculated theoretically, (17) becomes the evaluation of Ψ_{B}, which is shown in Fig. 2 for three typical measurement.

The Ψ_{B} factor is plotted against a normalized coordinate $\beta=h_0/h_i$ where h_i is the number of counts at channel i and h_0 is the maximum height of $g(i)$. It could be observed that Ψ_{B} is approximately constant above $\beta>20$. The three measurements differ in the detector resolution, which was artificically poored from run 3 to 1.

The above evaluation was made for the left-hand tail of the peak. The right-hand side could be analized in the same way but from calculation in standard measurements it is shown that the errors originated in

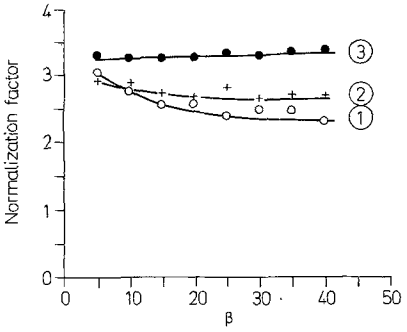

Fig. 2. Normalization factor vs. $\beta = h_0/h$ for three different runs. The detector resolution was reduces on purpose from run labelled *3* to *1*

the right-hand tail are smaller than those coming from the left-hand tail.
Summarizing,

$$\Delta(M_g^{(2)}) \sim |\delta(M_g^{(2)})| + \varepsilon_g^{\mathrm{B}} + \varepsilon_g^{\mathrm{A}} \tag{18}$$

with $\varepsilon_g^{\mathrm{A}} \ll \varepsilon_g^{\mathrm{B}}$. From now on, we shall not take into account the $\varepsilon_g^{\mathrm{A}}$ contribution. Besides if (9) and (11) are fulfilled, then $\delta(M_g^{(2)})$ is small enough as to ignore its calculation. The only remaining term is then $\varepsilon_g^{\mathrm{B}}$ which is computated through (14).

2.2. *Second-Moment Error Calculation of the Measured F(i) Distribution*

Now, we need to evaluate $\Delta(M_F^{(2)})$ taking into account statistical and systematic errors.
For the first case it is easy to see that the width of $F(i)$ is more or less twice that of the $g(i)$ distribution if both have the same shape. Then,

$$\delta(M_F^{(2)}) \simeq 2\,\delta(M_g^{(2)}) \tag{19}$$

and conditions (9) and (11) are also valid to minimize $\delta(M_F^{(2)})$.
The remaining systematic error contribution (ε_F) is, however, not so easy to handle, due to the fact that $F(i)$ emerges from (3). Following the same procedure as in Sect. 2. 1a) ε_F could be expressed as

$$\varepsilon_F = M_F^{(2)} - \hat{M}_F^{(2)} = \sum_{-\infty}^{\infty} F(i) i^2 - \sum_{-\mathrm{B}}^{\mathrm{A}} F(i) i^2 . \tag{20}$$

Now we need a mathematical expression for $F(i)$ outside of the $(-\mathrm{B}, \mathrm{A})$ interval. It will be given by the convolution of $g(i) \sim \exp(-\lambda i)$ with the intrinsic distribution $f(i)$ (inverted parabola) given by

$$f(i) = h_0[1 - (i/i_0)^2], \tag{21}$$

with h_0 defined as above. Of course, at this point we have neglected the Gaussian tails of $f(i)$. A further simplification suggests to approximate the parabola to a constant, h, defined between $\pm i_0$ then

$$h \sum_{j=-\infty}^{\infty} f(j-i)\,\mathrm{e}^{-\lambda j} = h\,\mathrm{e}^{-\lambda i} \sum_{k=-i_0}^{i_0} \mathrm{e}^{\lambda k}$$

$$= 2h\,\mathrm{e}^{-\lambda i} \frac{\mathrm{sh}\,\chi_0}{\lambda}, \quad k = i - j, \tag{22}$$

where $\chi_0 = i_0 \lambda$. The normalized contribution considering $F(i)$ between (B, ∞) will be

$$2\,\mathrm{e}^{-\lambda i} \frac{\mathrm{sh}\,\chi_0}{\chi_0}. \tag{23}$$

Now, applying (20) and using (23) for $F(i)$ we get

$$\varepsilon_F = \Psi \frac{\Psi \eta(\chi_F) S(\chi_0)}{\sigma_F} \tag{24}$$

with $S(\chi_0) \sim 2\,\mathrm{sh}(\chi_0)/\chi_0$ and $\chi_F = \lambda i_{\mathrm{B}}^F$.
Again we neglect the contribution of the right-hand side to ε_F. Then (24) will be properly defined as $\varepsilon_F^{\mathrm{B}}$, as above.

2.3. *Second-Moment Error Calculation of the Intrinsic f(i) Distribution*

From (5) we get

$$\Delta M_f^{(2)} \cong \Delta M_F^{(2)} - \Delta M_g^{(2)} . \tag{25}$$

Then using (14) and (24) and taking into account that $\sigma_F \sim \sigma_g \sqrt{511/E_g}$, where E_g is the energy of the response function, we get

$$\Delta M_f^{(2)} \simeq \frac{\Psi}{\sigma_g} \left[\eta(\chi_F) \sqrt{\frac{E_g}{511}}\, S(\chi_0) - \eta(\chi_g) \right]. \tag{26}$$

From our estimations the main contribution to $\Delta(M_f^{(2)})$ came from taking a finite interval in the distribution. This means that the $M_f^{(2)}$ should be corrected for a systematic errors, using (26) (Fig. 3).
The results for the η function are shown in Fig. 1. The dashed line represents the relation between h_0 and S and means that only the upper side of the plane is available if (8) and (9) are taking into account. From intersection of the η curve (labelled a) with the dashed line it could be established that a number of counts higher than 10^5 should be measured in order to have moderate errors according to (24) under typical measurement conditions.

2.4. *Higher-Order-Moments*

Similar calculations for higher-order moments could be done. In Fig. 1 the results for the η function (Curve *b*) of the fourth-order moment is shown. The intersection with the dashed line points out the required height of the measured peak (the dashed line for

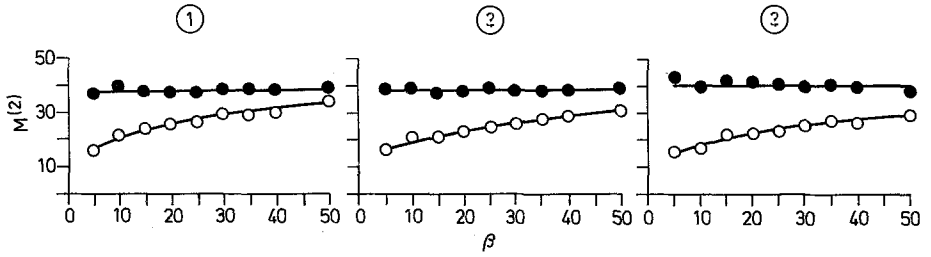

Fig. 3. Second-order moment of the measured distribution for the same runs as in Fig. 2. *Open circles:* Second-order moment of the distribution corresponding to 511 keV after subtracting the second-order moment corresponding to the response of the detector to monochromatic gamma-ray (662 keV of the ^{137}Cs in this case). *Solid circles:* Second-order moment after adding the $\Delta M_f^{(2)}$ correction. The resolution variations for the three compared spectra runs from 10 to 20%

the fourth-order moment lies parallel above and near the plotted line). It can be seen that now we need more than 10^7 counts to limit the errors.

3. Results and Conclusions

In order to prove the reliability of (26) the Doppler-broadened annihilation gamma ray line shape has been measured for Cu at room temperature using a 1.8 keV resolution Ge(Li) detector. The 662 keV gamma ray of ^{137}Cs was selected in order to reduce the perturbation of $g(i)$ over $F(i)$, then $g(i)$ has been measured simultaneously.

To obtain the parameters of the 662-keV gamma ray, the ANPIK code [9] was used. For monochromatic gamma rays this code assumes the same components we propose in Sect. 1. The experimental data are fitted to the proposed $g(i)$ distribution through the χ^2 test. Background subtraction for the 511- and 662-keV distributions were made fitting straigth lines up to ten $(\sigma^2)^{1/2}$ from left- and right-hand side to the center of the peak where both lines matched smoothly.

After subtracting the background from the original data in both measured peaks they were considered as $F(i)$ and $g(i)$, respectively. The curves shown in Figs. 2 and 3 were obtained using these data processed as was explained in the preceeding subjection.

The present results show that the $(-B, A)$ interval should be carefully determined in order to reduce the systematic errors introduced by not considering the distribution ranging from $-\infty$ to $+\infty$. The experimental evaluation of $\Delta M_f^{(2)}$ depends on the detector resolution, the background subtraction, the slope of the tails, the counting rate, and so on, although it behaves nearly as predicted by (26). In Fig. 3 the experimental results are shown. Open and solid circles are $M_f^{(2)}$ before and after the correction for the systematic error (which represents the main contribution to $\Delta M_f^{(2)}$). It is seen that a better detector resolution minimizes the correction for the systematic error.

Summarizing, from the error analysis of the second-order moment Eqs. (9), (11), and (26) were obtained. In (9) the maximum height of the $g(i)$ distribution is obtained for each order of the moments as a function of the detector characteristics (λ in this case). Equation (11) sets the number of keV/ channels to be used in order to minimize the error when the theoretical continuous distribution is considered as a discrete one. This was obtained as a function of the detector resolution and the precision (ε) fixed externally. Finally, (26) provides an estimation of the systematic error introduced by considering distribution not extended between $\pm\infty$.

From this analysis we conclude that the second-order moment provides reliable results if the errors are correctly evaluated and if the proper correction for systematic error is made, through (26). Higher-order moment error evaluation suggests that the number of counts collected should be very high in order to give reliable information (as high as in an angular correlation experiment).

References

1. R.N. West: Adv. Phys. 22, 263 (1973)
I. Ya Dekhtyar: Phys. Rep. **90**, 243 (1974)
2. P. Hautojärvi (ed.): *Positrons in Solids*, Topics Current Phys. **12** (Springer, Berlin, Heidelberg, New York 1979)
3. V.I. Goldanskii, K. Petersen, V.P. Shantarovich, A.V. Shishkin: Appl. Phys. **16**, 413 (1978)
4. K. Shizama: Nucl. Instrum. Methods **150**, 447 (1978)
5. R.M. Singru, K.B. Lal, S.J. Tao, R.M. Lambrecht: At. Data Nucl. Data Tables **20**, 475 (1977)
6. S.J. Tao: Appl. Phys. **16**, 409 (1978)
7. H. Cramér: *Mathematical Methods of Statistics* (Princeton University Press, Princeton, NJ 1961)
8. W.F. Sheppard: London Math. Soc. **29**, 353 (1898)
9. E. Achterberg: PhD Thesis, Physic Department, CNEA (available on request)